PHYSICAL REVIEW A VOLUME 44, NUMBER 3 1 AUGUST 1991

High-resolution K-shell photoabsorption measurements of simple molecules

Y. Ma,* C. T. Chen, and G. Meigs
AT&T Bell Laboratories, Murray Hill, New Jersey 07974

K. Randall
Fritz-Haber Institute, Berlin, Germany

F. Sette
AT&T Bell Laboratories, Murray Hill, New Jersey 07974

(Received 19 March 1991)

K-shell photoabsorption spectra of CO, $^{13}C^{18}O$, NO, O_2, CO_2, N_2O, C_2H_2, C_2D_2, C_2H_4, C_2D_4, C_2H_6, C_2D_6 measured with unprecedent energy resolution and signal-to-noise ratio are presented. These spectra reveal many new features in core-excited valence and Rydberg states. Detailed vibrational structures are observed in these spectra, providing valuable information on the geometrical and vibrational properties of the core-excited molecules. In addition, C 1s and N 1s core-hole lifetimes are found to be ~120 and ~135 meV in these molecules with little dependence on their bonding environments. These results and the tentative peak assignments are discussed briefly in terms of the equivalent core model, multielectron excitations, exchange interactions, and the geometry of the excited molecules.

I. INTRODUCTION

The inner-shell absorption spectra of molecules are one of the most fundamental probes of their electronic and geometric structures. The absorption spectra are also a prerequisite to the understanding of other molecular processes such as the photodissociation, electronic, or radiative deexcitation processes. Inner-shell absorption measurements also provide a testing ground for various molecular calculation schemes because they directly probe highly excited states of molecules. Due to the localized nature of the core levels, the inner-shell absorption spectra also represent different regimes of various interactions, such as the vibronic interaction in the molecules, as compared to the photoexcitation involving the more extended valence electrons. However, in spite of intense effort over the past 20 years [1], the inner-shell spectra of molecules have not been thoroughly investigated. This has been due to the lack of intense excitation sources that have both a high beam flux and an energy resolution that is better than the intrinsic lifetime width and vibrational spacings of the molecules. The development of new generation of soft-x-ray synchrotron-radiation monochromators, exemplified by the AT&T Bell Laboratories' Dragon beamline at the National Synchrotron Light Source [2] (NSLS), promises to revitalize this research field. In two previous studies we have used the Dragon beamline to study the N K shell of N_2 and the C $1s \rightarrow \pi^*$ excitations of benzene and ethylene [3,4], demonstrating the capability of the beamline and the rich information that can be obtained with its high-energy resolution.

In this paper we present inner-shell absorption measurements of CO, CO_2, C_2H_2, C_2H_4, C_2H_6 (carbon K shell), NO, N_2O (nitrogen K shell), and O_2 (oxygen K shell) molecules. Isotopes $^{13}C^{18}O$, C_2D_2, C_2D_4, C_2D_6 are also measured to identify the vibrational structures in the absorption spectra. All of the spectra were measured at the Dragon beamline with unprecedented photon energy resolution and signal-to-noise ratio. As will be discussed in the following sections these spectra provide valuable information on the core-hole lifetimes, exchange interactions, the excited-states geometry, vibronic interactions, and the validity of the equivalent core model [5,6] (ECM).

II. EXPERIMENT

The design and performance of the Dragon beamline has been discussed previously [2]. For the spectra presented in this paper, the photon-energy resolution was set at about 30–40 meV at the C K edge (~290 eV), 40–60 meV at the N K edge (~400 eV), and 60–80 meV at the O K edge (~540 eV). The absolute photon energy was calibrated against the strongest features observed in published electron-energy-loss spectroscopy (EELS) spectra [7–12]. Since the EELS peaks used for calibration are often composed of many individually resolved peaks in our high-resolution spectra, the uncertainty of the absolute energy position is ~0.2 eV. The relative energy positions within each spectra, however, are accurate within ~10 meV.

The photoabsorption spectra were measured with a 10-cm-long gas cell which was separated from beamline vacuum by 1200-Å-thick Ti (for C and N K shells) or Al (for O K shell) windows [3]. The transmitted photons were monitored by collecting photoelectrons generated from a gold target. The pressures of the gasses, ranging from ~0.05 Torr for the strongest absorption features to ~1 Torr for the weak features, were selected to minimize the saturation effect. Spectra taken with the empty cell were used to correct for the carbon and oxygen contamination on the reflecting surfaces of the beamline optics and on the windows.

III. RESULTS AND DISCUSSIONS

A. Carbon *K* shell of CO and $^{13}C^{18}O$

In a previous publication we presented high-resolution nitrogen *K*-shell data of N_2 [3]. With the much improved photon-energy resolution and data statistics, many new excitation lines were observed and high-precision spectroscopic constants, including term value, vibrational frequency, and internuclear separation, were deduced. By comparing with the optical-transition data of NO, we determined the final-state configuration of the 1*s* excited Rydberg states of N_2. The core-hole localization picture and the ECM are found to be valid to a high degree. The comparison between the Rydberg states in the C *K* shell of CO and in the N *K* shell of N_2 is of particular interest. Since the core excited Rydberg states of CO and N_2 have the same final states in the ECM as the 2π valence-excited Rydberg states of NO, one would expect very similar Rydberg transitions for these two molecules.

In Fig. 1, we show (a) the *C* $1s \rightarrow 2\pi^*$, (b) C $1s \rightarrow$Rydberg states, and (c) the double-excitation spectra for CO and $^{13}C^{18}O$. As is clearly seen, isotope shifts of as small as 20 meV are observed (with ~300-eV excitation

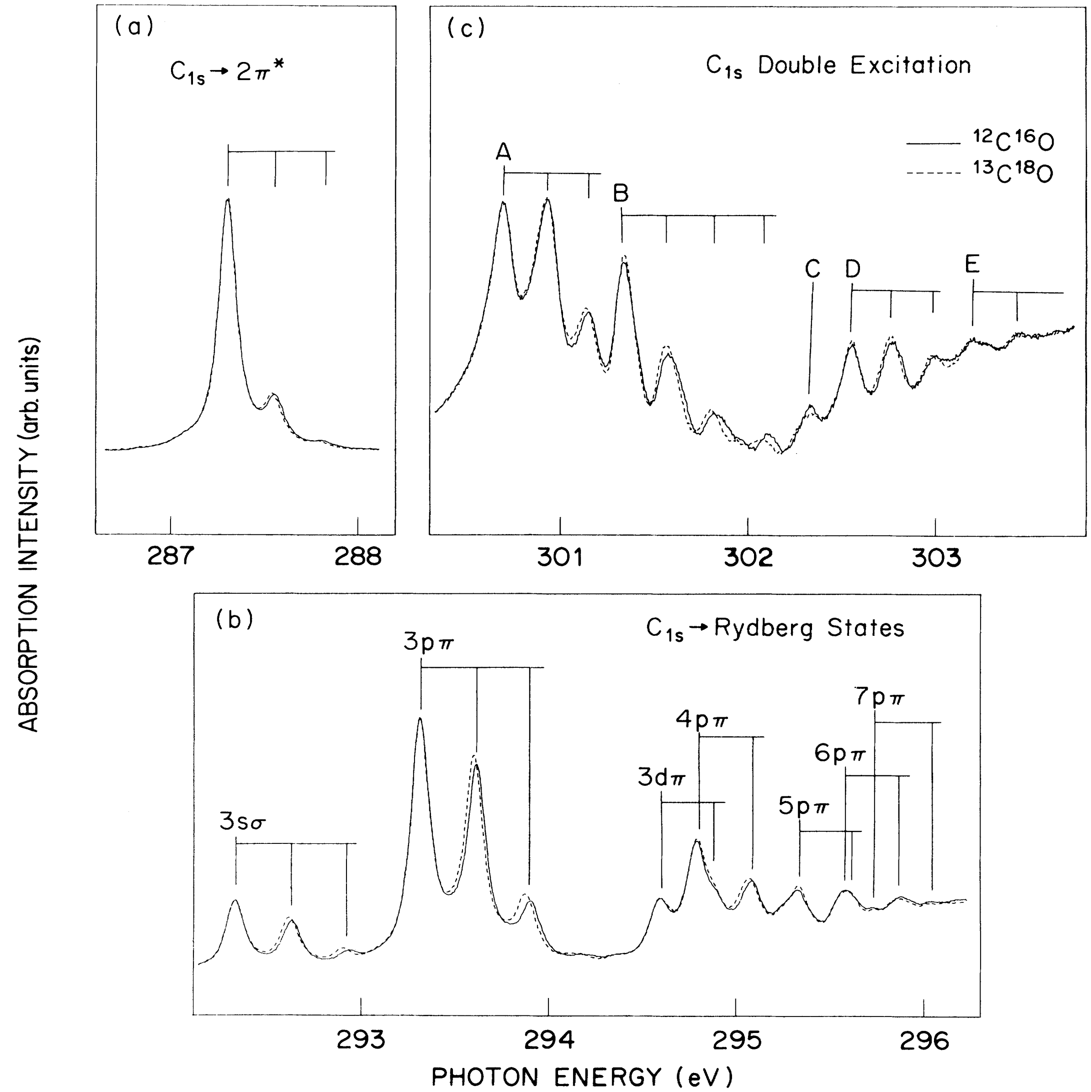

FIG. 1. Carbon *K*-shell photoabsorption spectra of CO (solid line) and $^{13}C^{18}O$ (dashed line): (a) C $1s \rightarrow 2\pi^*$ (b) *C*$1s \rightarrow$Rydberg states, and (c) the double-excitation region.

energy), in agreement with the calculated shift of ~0.09$\hbar\omega$. The observation of such small changes in the spectra underlines the capability of the Dragon beamline and points to new opportunities for inner-shell absorption studies.

The isotope shifts observed in these spectra aid the identification of different vibrational series [6]. The intensities of vibrational sidebands observed here are much different from those of N_2, due to the difference in the internuclear separation between the ground and core-excited states of CO and N_2 (Refs. [6,13]).

Having identified the vibrational series in the spectra, the assignment of the Rydberg states is straightforward. Following the same procedure as that for N_2 (Ref. [3]), the peak assignment for the core-excited Rydberg states of CO are given in Fig. 1. Five electronic transitions in the double-excitation region are aslo identified. They are at *A*: 300.69; *B*: 301.34; *C*: 302.33; *D*: 302.55; and *E*: 303.19 eV. The assignment for these double excitations, however, is more difficult due to the complicated shake-up processes: the C $1s \rightarrow 2\pi$ transition is accompanied by the excitation of a second electron from one of the valence orbitals, 1π or 5σ, to the 2π or the Rydberg states. Theoretical calculations are needed to identify their electronic configurations.

In Fig. 2 we compare the Rydberg states spectra of CO and N_2, plotted as functions of term value, i.e. the difference between the ionization potential (V_{ion}) and transition energy ($h\nu$). The ionization potentials for N_2 and CO are 409.938 and 296.080 eV, respectively. This figure clearly shows that the term values $3s\sigma$, $3p\pi$, and $4p\pi$ states are essentially the same, demonstrating again the validity of the ECM.

The Rydberg states at around 1.5 eV, however, have term values differing by ~0.1 eV. This apparent breakdown of the ECM can be avoided by assigning different Rydberg states to these two peaks, i.e., $4s\sigma$ for N_2 and $3d\pi$ for CO. Thus we conclude that ECM is valid for transition energies, but the oscillator strengths can be very different. In fact, we also note that while all the $np\pi$ Rydberg states line up in these two spectra, none of the $Ns\sigma$ ($n > 3$) states of CO are visible.

The systematic differences can be attributed to two fundamental differences in these two equivalent core (EC) molecules: (1) N_2 has mirror-plane symmetry while CO does not; (2) the overlap between the $1s$ electron and the Rydberg-state wave functions is diffrent in the two molecules. For CO the core electron is excited from the N site of its equivalent-core–valence-excited NO molecule, while for N_2, it is excited from the O site. These differences in the oscillator strength should provide a stringent test for theoretical calculations and call for high-resolution measurements of the β parameters for the two states in question.

B. Nitrogen *K* shell of NO

The N $1s \rightarrow 2\pi^*$ and the N $1s \rightarrow$Rydberg-states spectra are shown in Figs. 3(a) and 3(b), respectively. Compared

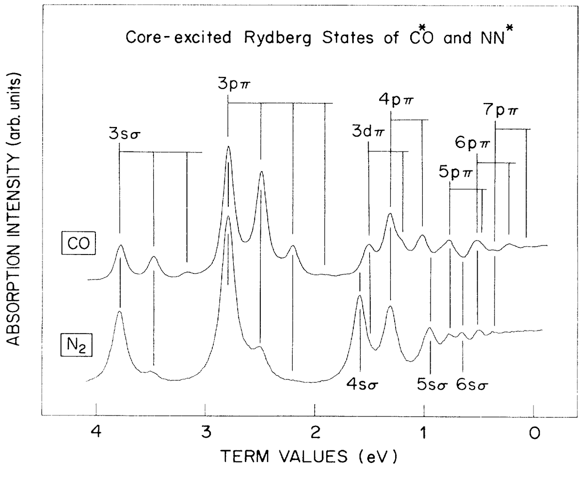

FIG. 2. Comparison of the Rydberg states of the carbon K shell of CO and the nitrogen K shell of N_2.

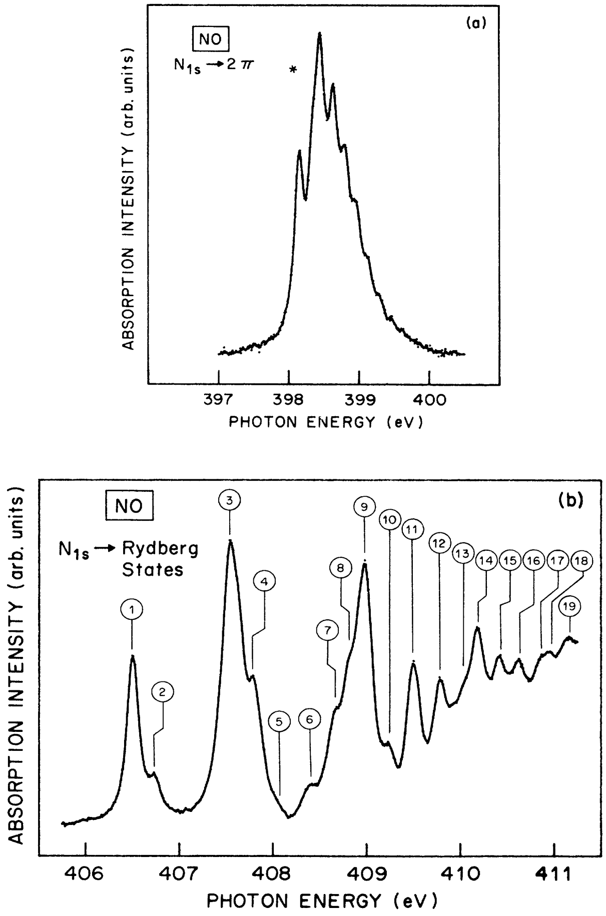

FIG. 3. Nitrogen *K*-shell photoabsorption spectrum of NO: (a) N $1s \rightarrow 2\pi^*$ and (b) N $1s \rightarrow$Rydberg states.

TABLE I. N *K* shell of NO; *v* represents vibrational structures.

Peak No.	Position	Term[a]	Term[b]	Assignment $^3\Pi$	$^1\Pi$
1	406.60	3.70		$3s\sigma$	
2	406.83				
3	407.65	2.65	4.15	$3p\pi$	
	~407.75[c]	2.55	4.05	$3p\sigma$	
4	407.88	2.42	3.92		$3s\sigma$
5	~408.15	2.15	3.65		
6	408.51	1.79	3.29	$4s\sigma$	
7	408.77	1.53	3.30	$3d\pi$	
8	408.92	1.38	2.88	$4p\pi$	
9	409.08	1.22	2.72		$3p\pi$
10	409.34	0.96	2.46	$5s\sigma$	
11	409.60	0.70	2.20	$5p\pi$	
12	409.88	0.42	1.92	$6p\pi$	
13	~410.14		1.66		
14	410.28		1.52		$4s\sigma$
15	410.52		1.28		$4p\pi$
16	410.72		1.08		$3d\pi$
17	~410.97		0.83		$5s\sigma$
18	~411.05		0.75		$5p\pi$
19	411.25		0.55		$6p\pi$

[a] Using $V_{\text{ion}}=410.3$ eV (Ref. [15]) for the $^3\Pi$ ionic state.

[b] Using $V_{\text{ion}}=411.8$ eV (Ref. [15]) for the $^1\Pi$ ionic state.

[c] Obtained from curve fitting.

to the closed-shell electronic configuration of N_2 and CO, the NO molecle has one more electron in the 2π orbital. Consequently, the absorption spectra show more complicated structures.

The N $1s \rightarrow 2\pi^*$ transition has four final states, three of them ($^2\Sigma^-, ^2\Delta^-, ^2\Sigma^+$) are dipole permitted [8,12]. Judging from the spectrum in Fig. 3(a), only two vibrational series have significant intensities. Our preliminary analysis shows that this spectrum can indeed be satisfactorily fitted with only two vibrational series. The intensity ratio of the two transitions is found to be roughly 2:3 with energy separation of 0.3 eV.

The analysis also gave a Lorentzian lifetime width of 135 meV and a vibrational spacing of 190 meV. The lifetime width is very similar to that of N_2, despite the differences in valence-electron configuration between these two molecules [14]. The 190-meV vibrational spacing is much smaller than that in the N $1s^{-1}1\pi_g^*$ state of N_2 (235 meV) due to the weakening in the bond strength by the extra 2π antibonding electron. This vibrational spacing is very similar to the ground-state stretching frequency, 196 meV, of the equivalent core molecule O_2, demonstrating the validity of the ECM.

The Rydberg states in Fig. 3(b) show some resemblance to those of N_2 and CO shown in Fig. 2. Because of the exchange interaction between the photoelectron and the 2π electron, there are two dipole-allowed Rydberg series [7]; one converges to the ionic state $^3\Pi$ and the other to $^1\Pi$. The peak positions observed in Fig. 3(b) and their possible assignments are listed in Table I. The assignment given here is based on Ref. [7] and the term values of N_2.

The first few peaks in Fig. 3(b) were analyzed using curve fitting. For peak Nos. 1 and 2, a Lorentzian lifetime width of 133 meV and a vibrational spacing of 230 meV are obtained. This spacing is again smaller than the ~300 meV found for the Rydberg states of N_2 (Ref. [3]). In fitting peaks 3 through 5, we included an extra unresolved peak, whose presence can be justified by the broad profile of peak 3. This gave the position of the unnumbered peak in Table I. No fitting was attempted for other peaks in the spectrum because of the complication of many unresolved peaks.

From our assignment, an exchange splitting of 1.3 eV is obtained for the $3s\sigma$ singlet and triplet states, and 1.4 eV for $3p\pi$ states. These values approach the exchange splitting of the ionic states (1.5 eV) [15], as expected.

C. Oxygen *K* shell of O_2

The O *K*-shell spectra are shown in Fig. 4. The $O1s \rightarrow 1\pi_g^*$ transition, at about 521 eV in Fig. 4(a), is a single broad peak with width ~1.5 eV, confirming earlier EELS measurements [11]. This broad peak is due to the unresolved vibrational levels with the frequency comparable to the O 1*s* core-hole lifetime.

The Rydberg-states spectra of O_2, shown in Fig. 4(b), are qualitatively different from those of N_2 and NO. The major difference is the two broad features near 539 and 542 eV. These features were originally assigned to $3s\sigma$

TABLE II. O K shell of O_2; v represents vibrational structures.

Peak No.	Position	Term[a]	Term[b]	Assignment $^4\Sigma$	$^2\Sigma$
1	539.05	4.05		$3s\sigma_g$	
2	~539.32	3.78		v	
3	~539.54	3.56	4.66	σ^*	
4	540.25	2.85	3.95	$3p\pi_u$	$3s\sigma_g$
5	~540.74	2.36	3.46	$3p\sigma_u$	
6	~540.94	2.16	3.26	v	
7	541.16	1.94	3.04	$3d\pi_u$	
8	541.35	1.75	2.85	$4s\sigma_g$	$3p\pi_u$
	~541.8[c]	1.3	2.4		σ^*
9	541.85	1.25	2.35	$4p\pi_u$	$3p\sigma_u$
10	~542.03	1.07	2.17	$4p\sigma_u$	
11	542.28	0.82	1.92	$5p\pi_u$	$3d\pi_u$
12	542.52	0.58	1.68	$6p\pi_u$	$4s\sigma_g$
13	542.75	0.35	1.45	$7p\pi_u$	
14	~543.18		1.02		$5s\sigma_g$

[a] Using $V_{\text{ion}} = 543.1$ eV (Ref. [17]) for the $^4\Sigma$ ionic state.
[b] Using $V_{\text{ion}} = 544.2$ eV (Ref. [17]) for the $^2\Sigma$ ionic state.
[c] The position of the broad peak.

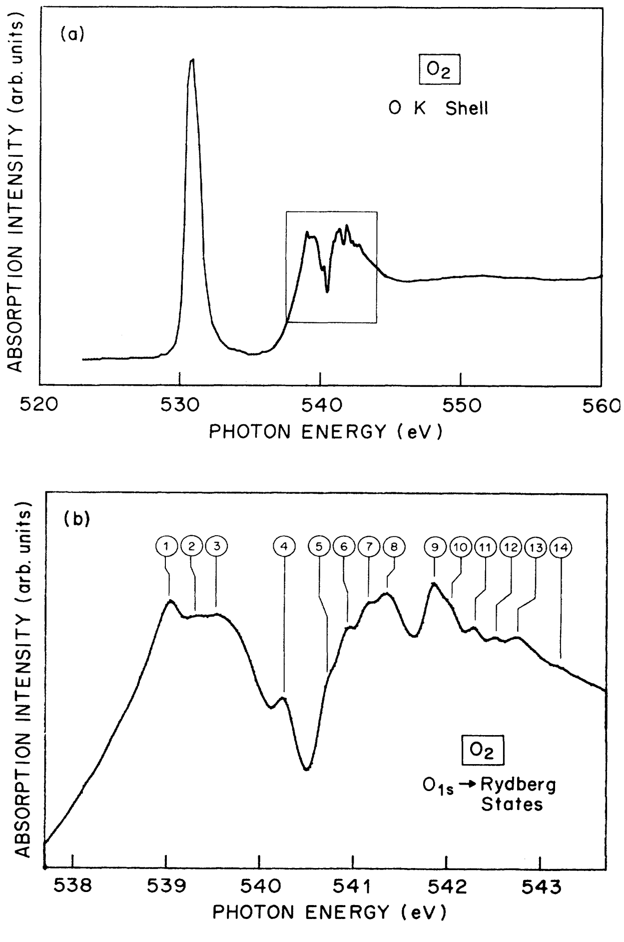

FIG. 4. (a) Oxygen K-shell photoabsorption spectrum of O_2. (b) The Rydberg-states region, shown boxed in (a), is expanded.

and $3p\pi$ Rydberg states [11]. Our high-resolution measurement, however, resolved many fine structures in this region. The positions of these peaks are listed in Table II, together with our *tentative* assignment. The assignment is based on the similarity between the term values with those of NO and N_2, and on the theoretical results of Gerwer *et al.* [16]. Similar to the case of NO, there are two dipole-allowed Rydberg series [7], one converging to the ionic state $^4\Pi$, and the other to $^2\Pi$. Based on the assignment given in Table II, the exchange splittings between the Rydberg states in the two series is ~1.1 eV, close to the exchange splitting of the ionic states [17].

This observation of the Rydberg states is consistent with the assignment of the two broad features at ~539.5 and ~541.8 eV eV as the exchange split $2p\sigma_u^*$ resonances, pulled down from the continuum to below the ionization threshold by a strong attractive shape resonance [18]. The exchange splitting for the $2p\sigma_u^*$ resonances, however, is ~2.3 eV, much larger than the exchange splitting of ~1.1 eV found for the Rydberg states, and the calculated value of 1.4 eV [18]. Clearly, more investigations are needed to find reasons for this large difference and to suggest other possible assignments for the Rydberg states.

Peak No. 2 in Fig. 4 is assigned to vibrational excitation. This gives a O-O stretching frequency of ~270 meV in this Rydberg state, much larger than the 196 meV for the ground state.

D. Carbon K shell of CO_2

The C $1s \rightarrow$Rydberg state spectrum is shown in Fig. 5 and peak positions are listed in Table III. The C $1s \rightarrow 2\pi_u^*$ spectrum (not shown) exhibits a ~0.6-eV-wide broad peak similar to that observed in the EELS measurement [8,10]. The broadening has been attributed to

TABLE III. C K shell of CO_2; v represents vibrational structures.

Peak No.	Position	Term[a]	Assignment	NO_2[b]	Theory[c]
1	292.74	4.97	3s	3.7	5.0
2	292.86	4.85	v		
3	~292.95	4.76	v		
4	293.09	4.62	v		
5	294.96	2.75	3p	2.6	2.6
6	295.15	2.56	v		
7	~295.33	2.38	v		
8	295.63	2.08	3d	~1.8	
9	~296.16	1.55	4s	1.5	2.0
10	296.38	1.33	4p	1.2	1.2
11	296.56	1.15	v		
12	296.91	0.80	5p		
13	297.15	0.56	6p		

[a] Using $V_{\text{ion}}=297.71$ eV (Ref. [19]).
[b] Reference [20].
[c] Reference [21].

the unresolved low-energy bending mode and supports the notion that CO_2 in the core-excited state is bent [8]. This is not unexpected since its equivalent core molecule NO_2 is bent in ground state.

The difference in geometry between CO_2 (linear) and its equivalent core molecule NO_2 (bent) also causes large differences in their respective term values for the Rydberg states. This is evident from Table III where we compare the term values for CO_2 with those of the $6a_1$ excited states of NO_2 [20]. Among them, the disagreement betwen the 3s states is especially large. When one takes into account the difference in geometry as well as the difference in exchange interaction of the two systems [21], the ECM is found to be still valid. The results of the calculation as well as the peak assignments are also listed in Table III.

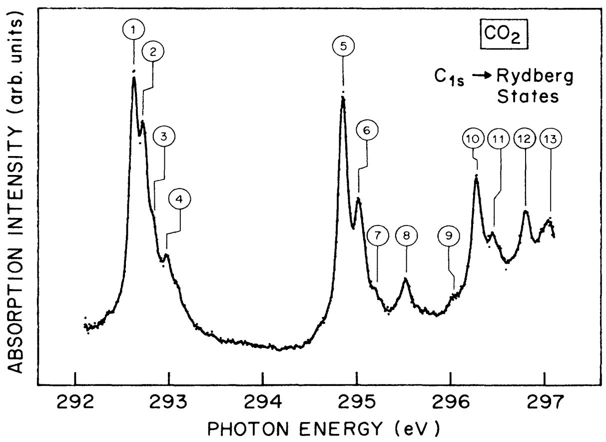

FIG. 5. Carbon K-shell photoabsorption (Rydberg states) spectrum of CO_2.

Several vibrational lines are observed in the spectrum. Guided by the ground-state vibrational frequencies of 168 meV for the symmetric stretch, 83 meV for the bending, and 297 meV for the antisymmetric stretch, the 190-meV separation between peak Nos. 6 and 5, is assigned to the symmetric stretching mode. Similarly, peak No. 11 is assigned to the symmetric stretch mode associated with the 4p electronic transition. The vibrational structure of the 3s state, however, shows very different behavior. The energy separation between peak No. 2 and the 3s state is only 120 meV. The most plausible assignment for peak No. 2 is the symmetric stretch sideband of the 3s state. The much reduced frequency, however, suggests that the 3s state has a substantial antibonding charcter. Peak No. 3, weak and separated by ~210 meV, is probably an overtone of the symmetric stretch, while Peak No. 4 is the antisymmetric stretching mode. If this is indeed the case, we then have a much increased vibrational spacing, ~350 meV compared to 297 meV in the ground state for the antisymmetric stretch, while the symmetric stretching frequency is reduced, 120 versus 168 meV [6]. By curve fitting the 3s and 3p peaks, the C 1s lifetime width is found to be about 120 meV, similar to that of core-excited CO, ethylene, and benzene [4].

E. Nitrogen K shell of N_2O

N_2O is also a linear molecule and is isoelectronic to CO_2. However, the N K shell spectra shown in Fig. 6 are quite different from those of CO_2. This is due to the two inequivalent nitrogen atoms, terminal (N_t) and center (N_c), in this molecule. The two most prominent peaks in Fig. 6(a) have been identified as the $N_t 1s \rightarrow 3\pi$ and the $N_c 1s \rightarrow 3\pi$ transitions [8,11]. Similar to the case of CO_2, these peaks are very broad, indicating the strong excitation of the low-energy bending mode, and suggesting that the molecule is bent not only in the $(N_t 1s)^{-1}3\pi$ state but also in the $(N_c 1s)^{-1}3\pi$ state.

The positions of the Rydberg states and their assignments are listed in Table IV. The assignment was based on the term values of N_2, and the fact that N_t core-excited Rydberg states, N*NO, are similar to C core-excited CO_2 OC*O. These peak assignments are tentative and inconclusive. For instance, although it is dipole unfavored, based on term values consideration, the most intense peak, No. 4 in Fig. 6(b), is assigned to the N_t core-excited 3*d* state. Aternatively, we may assign this peak to the N_c core-excited 3*s* state, but then the 6.1-eV term value is much higher than the ~4 eV typically found for the 3*s* states in all other molecules.

Peak No. 11–15 and No. 17–20 are equally spaced (160–170 meV); therefore, they are clearly of vibrational origin. These energy spacings are close to the 159 meV of the N-O stretch in the ground state. The strong N-O stretch vibrational sideband indicates that the N-O distance has been greatly modified in these Rydberg states.

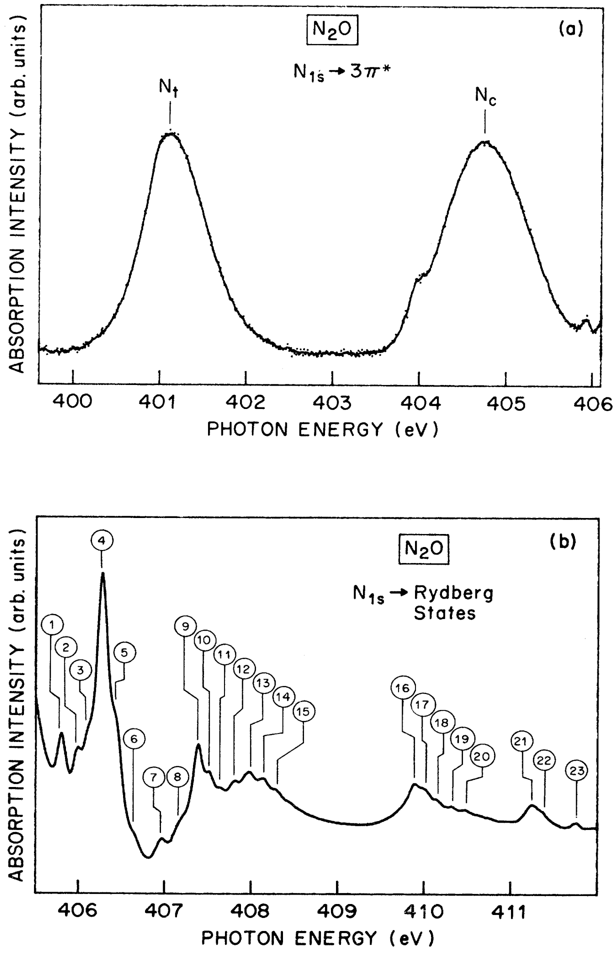

FIG. 6. Nitrogen *K*-shell photoabsorption spectrum of N_2O. (a) N $1s \rightarrow 3\pi^*$ and (b) the Rydberg region.

Other peaks in Fig. 6(b), e.g., peak 2, 3, 5, 10, and 22, are also very likely due to vibrational excitations. A more conclusive identification of these vibrational structures should be achievable with the combination of theoretical calculations and isotope measurements. Since N 1*s* electrons are localized on either the terminal or the central nitrogen, a conclusive identification of these vibrational structures should offfer valuable information regarding the local bonding and vibrational properties of the molecule.

F. Carbon *K* shell in C_2H_2 and C_2D_2

Acetylene is a linear molecule which is isoelectronic to N_2. The C $1s \rightarrow \pi^*$ and the C $1s \rightarrow$Rydberg states are shown in Figs. 7(a) and 7(b), respectively. Similar to the

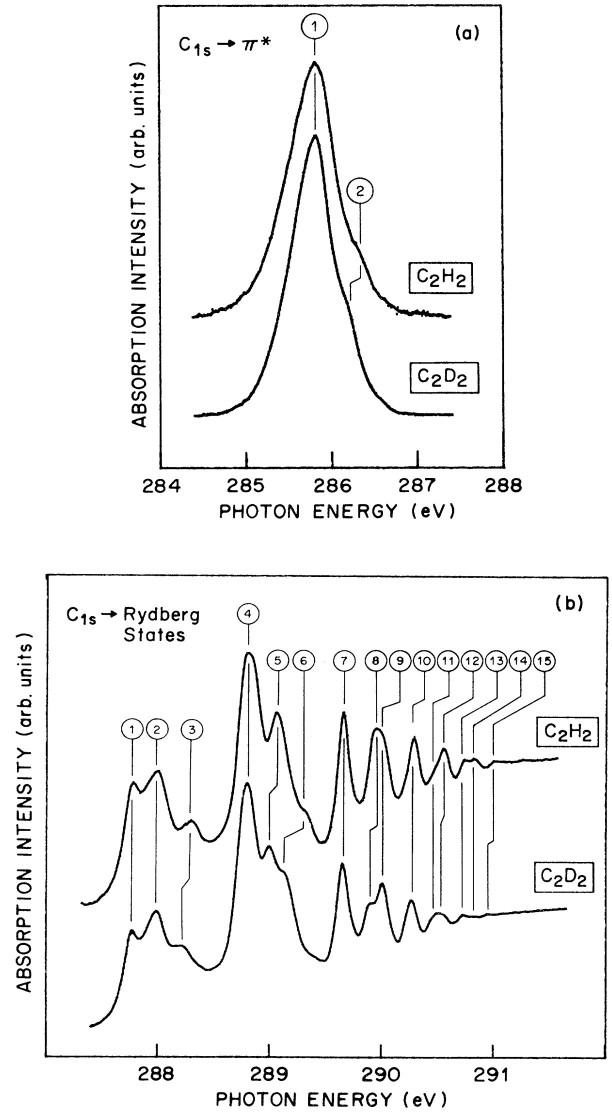

FIG. 7. Carbon *K*-shell photoabsorption spectra of C_2H_2 and C_2D_2. (a) C $1s \rightarrow 2\pi^*$ region and (b) C $1s \rightarrow$Rydberg-states region.

TABLE IV. N *K* shell of N_2O; *v* represents vibrational structures.

Peak No.	Position	Term[a]	Term[b]	Assignment	
				N_t	N_c
	404.00	4.50		3*s*	
1	405.91	2.60		3*p*	
2	406.09	2.41		*v*	
3	~406.21	2.29		*v*	
4	406.37	2.13	6.13	3*d*	
5	~406.53	7.97	5.97	*v*	
6	~406.77	1.73	5.73	*v*	
7	407.07	1.43	5.43	4*s*	
8	~407.29	1.21	5.21	4*p*	
9	407.49	1.01	5.01		3*s*
10	407.68	0.88	4.88	5*s*	
11	407.75	0.75	4.75	5*p*	3*p*
12	407.91	0.59	4.59		*v*
13	408.07	0.43	4.43		*v*
14	408.24	0.26	4.26		*v*
15	408.40		4.10		*v*
16	409.99		2.51		3*p*
17	410.09		2.41		3*d*+*v*
18	410.24		2.26		*v*
19	410.42		2.08		*v*
20	410.57		1.93		*v*
21	411.35		1.15		4*p*
22	~411.45		1.05		5*s*
23	411.85		0.65		6*s*

[a] Using $V_{\text{ion}}=408.5$ eV (Ref. [17]) for terminal N.
[b] Using $V_{\text{ion}}=412.5$ eV (Ref. [17]) for centered N.

cases of the other linear molecules, CO_2 and N_2O, the C $1s \rightarrow \pi^*$ peak is very broad, indicating the excitation of low-energy bending modes. Only a shoulder, which shifts with the isotope substitution, is discernible in the spectra. It is therefore associated with the C-H (C-D) stretching modes. The strong excitation of the bending modes again suggests that the molecule in the excited state is bent. We believe that this is due to the similar rehybridization process that has been proposed to explain the observation of symmetry breaking in the C $1s \rightarrow \pi^*$ spectra of

TABLE V. C *K* shell of C_2H_2 and C_2D_2; *v* represents vibrational structures.

Peak No.	C_2H_2 position	C_2D_2 position	Term[a]	Assignment
1	287.74	287.73	3.36	3*s*
2	287.96	287.95	3.14	*v*(C-C)
3	288.26	288.19		*v*(C-H)
4	288.76	288.76	2.34	3*p*
5	289.02	288.96	2.08	*v*(C-H)
6	~289.27	289.10		*v*(C-H)
7	289.62	289.61	1.48	4*s*
8	~289.91	289.86	1.19	*v*
9	~289.96	289.97	1.14	4*p*
10	290.25	290.23	0.85	5*s*
11	~290.43	290.41	0.67	5*p*, 6*s*
12	290.52	~290.51	0.58	6*s*+*v*
13	290.70	290.69	0.40	6*p*
14	290.79	290.79	0.30	7*s*+7*p*+*v*
15	290.96	290.92	0.14	

[a] Using $V_{\text{ion}}=291.1$ eV (Ref. [22]) for C_2H_2.

ethylene and benzene [4], i.e., from the *sp* hybridization in the ground state to sp^2 hybridization in the C $1s^{-1}\pi^*$ state.

Aside from the vibrational structures, which are identified from the isotope shifts, the Rydberg spectra in Fig. 7(b) resemble those of CO and N_2 shown in Fig. 2. In fact, the assignment of the Rydberg states listed in Table V are based on this similarity. The term values are found to be very close to those of N_2, especially those of the higher Rydberg states. This is not surprising, considering the close similarity of C_2H_2 and N_2. Since the Rydberg orbitals have large radii, the energies of the Rydberg states are not much affected by the presence of the hydrogen atoms.

The lifetime width, as measured from the width of the 3*s* peak, is 170 meV. This width is substantially larger than the 110–120 meV found for CO, ethylene and benzene [4], and may have contributions from the unresolved low-energy bending modes.

Intense vibrational sidebands are observed for several Rydberg states. Based on isotope shifts, these sidebands are *tentatively* identified. The great difference observed in the vibrational structures of the 3*s* and 3*p* states suggests that these two Rydberg orbitals have a different effect on the C—C and C—H bonding. In particular, the C—C stretch mode is strongly excited in the 3*s* state but less so in the 3*p* states, indicating that the 3*s* Rydberg electron has a larger effect on the C—C bond strength than the 3*p* Rydberg electron does.

G. Carbon *K* shell of C_2H_2 and C_2D_4

The C 1*s*→Rydberg-states spectra are shown in Fig. 8. Many more peaks are observed than in the EELS studies [9,10]. The peak positions and *tentative* assignment are listed in Table VI. The C 1*s*→π^* spectra have been discussed elsewhere [4,23].

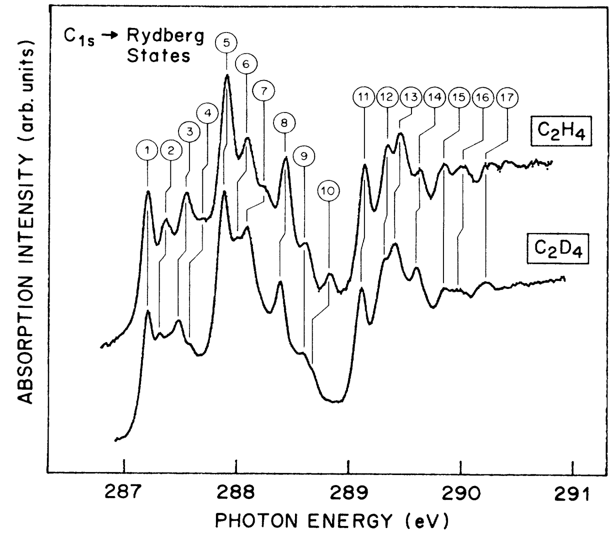

FIG. 8. Carbon *K*-shell photoabsorption spectra of C_2H_4 and C_2D_4.

Although ethylene is isoelectronic to O_2, its core-excited Rydberg states are much different from those of O_2. The spectrum is similar to that of the acetylene but with several differences: (1) the 3*s* and 3*p* states are closer, separated by only 0.7 eV, as compared to ~1 eV for N_2, NO, and acetylene; (2) an intense peak, No. 8, which has no counterpart in acetylene spectra, is assigned to the 3*d* state; (3) the 0→0 transition energies are slightly different in the two isotopes, e.g., the 3*s*-3*p* energy separation differ by ~20 meV between C_2H_4 and C_2D_4, due

TABLE VI. C *K* shell of C_2H_4 and C_2D_4; *v* represents vibrational structures.

Peak No.	C_2H_4	C_2D_4	Term[a]	Assignment
1	287.09	287.09	3.51	$3s\sigma$
2	287.25	287.20		v(C-H)
3	287.43	287.36		v(C-H)
4	~287.58	~287.48		v(C-H)
5	287.79	287.77	2.81	$3p\pi+3p\sigma$
6	287.97	287.89		v(C-H)
7	~288.13	287.97		v(C-H)
8	288.30	288.28	2.29	$3d$
9	288.49	288.48	2.11	v(C-H)
10	288.71	~288.60		v(C-H)
11	289.01	288.99	1.59	$4s\sigma$
12	289.22	289.22	1.38	$4p\pi+v$
13	289.32	289.30	1.28	
14	289.50	289.48	1.10	$5s\sigma$
15	289.73	289.73	0.87	$5p\pi$
16	~289.89	~289.87	0.71	$6s\sigma$
17	~290.13	~290.11	0.47	$6p\pi$

[a] Using $V_{\text{ion}}=290.6$ eV (Ref. [22]) for C_2H_4.

TABLE VII. C *K* shell of C_2H_6 and C_2D_6; *v* represents vibrational structures.

Peak No.	C_2H_6	C_2D_6	Term[a]	Assignment
1	286.80	286.80	3.8	3*s*
2	~286.95	~286.92		*v*(C-H)
3	287.13	287.06		*v*(C-H)
4	~287.30	~287.20		*v*(C-H)
5	287.83	287.84	2.77	3*p*
6	287.98	287.92		*v*(C-H)
7	288.17	288.05		*v*(C-H)
8	288.63	288.61	1.97	3*d*
9	~288.80	~288.73		*v*(C-H)
10	289.00	288.9	1.6	*v*
		289.0		4*s*
11	289.28	289.26	1.32	4*p*
12	289.46	~289.34		*v*(C-H)
13	289.67	289.54		*v*(C-H)
14	289.80	289.76	0.84	*v*+5*p*
15		290.04	0.56	*v*+6*p*

[a] Using $V_{\text{ion}} = 290.6$ eV (Ref. [24]) for C_2H_6.

to the differences in the zero-point vibrational energies $(1/2\Sigma\hbar\omega)$ [6,25].

Vibrational structures are observed in several Rydberg states. Comparing them to aceytlene, we note that the vibrational structures of the 3*p* peaks in these two molecules are very similar, while those of the 3*s* states are much different. In contrast to the case of acetylene, there is no strong C-C mode excitation in core-excited Rydberg states of ethylene. The lifetime width is found to be 120 meV, similar to the C $1s^{-1}\pi^*$ state [4].

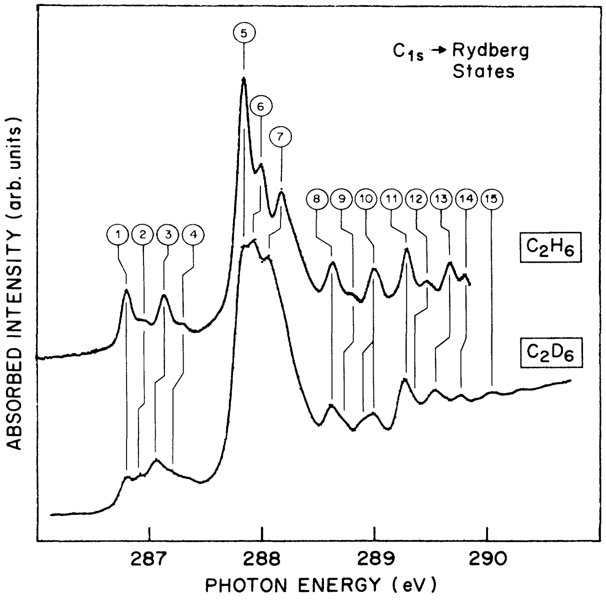

FIG. 9. Carbon *K*-shell photoabsorption spectra of C_2H_6 and C_2D_6.

H. Carbon *K* shell of C_2H_6 and C_2D_6

The C *K*-shell spectra are presented in Fig. 9 and the peak positions are listed in Table VII. The spectra are similar to those of the acetylene and ethylene, but the 3*s* to 3*p* intensity ratio is much weaker in ethane. This could be due to the fact that the ethane molecule is more isotropic than either ethylene or acetylene, and therefore the dipole transition from the C 1*s* to the Rydberg 3*s* orbital has a smaller amplitude. In this regard, the spectra in Fig. 9 are very similar to those of methane [26], where the 3*s* state is even weaker because the 1*s* to 3*s* transition is dipole forbidden and the observed oscillator strength is due to the vibronic coupling effect [26].

IV. CONCLUSIONS

Through systematic studies of the high-resolution inner-shell absorption spectra of molecules, from the simple CO and N_2 to polyatomic molecules, we found the following.

(1) All the Rydberg-states spectra are in general similar when the complications due to multiplet splitting, vibrational structures, and multiple-excitation sites are screened out. This greatly aids the Rydberg-states assignments.

(2) The exchange interaction and multielectron excitations can be studied in great detail, as shown in the cases of CO, NO, and O_2.

(3) Vibrational structures associated with valence and Rydberg states are ubiquitous in the inner-shell spectra. They show great variations among different valence and Rydberg states. This allows detailed studies of the vibrational and geometrical properties of the core-excited molecules. In particular, since the core excitation is localized, the vibrational excitation will also be highly localized. Therefore it should be possible to use the vibrational structures as a local probe of molecular vibrations.

(4) Symmetry breaking is commonly associated with the core excitation of many highly symmetric molecules, especially the linear molecules presented in this paper, CO_2, N_2O, and acetylene. Rehybridization of the orbitals appears to provide an explanation for this type of symmetry breaking. The importance of the vibronic interactions in these systems is currently under investigation [23].

(5) The C 1*s* and N 1*s* core-hole lifetime widths are found to be 120 and 135 meV, with little dependence on the local bonding environment [14].

(6) More thorough theoretical investigations are necessary for a better understanding of all the spectra.

With the increasing number of high-resolution soft-x-ray synchrotron-radiation beamlines now under construction, we believe that much more valuable information regarding core-excited molecules will be obtained by photoabsorption spectroscopy in the near future. The challenge now is for molecular calculations to catch up with the rapid experimental developments.

ACKNOWLEDGMENTS

We acknowledge stimulating discussions with A. M. Bradshaw and the excellent technical assistance of E. Chaban. This work is done at the National Synchrotron Light Source which is supported by the U.S. Department of Energy under Contract No. DE-AC02-76CH00016.

---

*Present address: National Synchrotron Light Source, Brookhaven National Laboratories, Upton, NY 11973.

[1] See, for example, A. P. Hitchcock, J. Electron. Spectrosc. **25**, 245 (1982); and unpublished.

[2] C. T. Chen, Nucl. Instrum. Methods A **256**, 595 (1987); C. T. Chen and F. Sette, Rev. Sci. Instrum. **60**, 1616 (1989); Phys. Scr. **T31**, 119 (1990).

[3] C. T. Chen, Y. Ma, and F. Sette, Phys. Rev. A **40**, 6737 (1989).

[4] Y. Ma, F. Sette, G. Meigs, S. Modesti, and C. T. Chen, Phys. Rev. Lett. **63**, 2044 (1989); Phys. Scr. **41**, 833 (1990).

[5] A preliminary account of these results has been presented by Y. Ma, C. T. Chen, G. Meigs, K. Randall, and F. Sette, in *X-Ray and Inner-Shell Processes, Knoxville, 1990,* Proceedings of the Conference on X-Ray and Inner-Shell Processes, AIP Conf. Proc. No. 215, edited by Manfred Krause and Thomas Carlson (AIP, New York, 1990), p. 634.

[6] C. T. Chen *et al.* (unpublished).

[7] G. R. Wight and C. E. Brion, J. Electron. Spectrosc. **4**, 313 (1974).

[8] G. R. Wight and C. E. Brion, J. Electron. Spectrosc. **3**, 191 (1974).

[9] A. P. Hitchcock and C. E. Brion, J. Electron. Spectrosc. **10**, 317 (1977).

[10] M. Tronc, G. C. King, and F. H. Read, J. Phys. B **12**, 137 (1979).

[11] A. P. Hitchcock and C. R. Brion, J. Electron. Spectrosc. **18**, 1 (1980).

[12] M. Tronc, G. C. King, and F. H. Read, J. Phys. B **13**, 999 (1980).

[13] M. Domke *et al.*, Chem. Phys. Lett. **173**, 122 (1990).

[14] M. Coville and T. D. Thomas (unpublished).

[15] D. W. Davis and D. A. Shirley, J. Chem. Phys. **56**, 669 (1972).

[16] A. Gerwer, C. Asaro, B. V. McKoy, and P. W. Langhoff, J. Chem. Phys. **72**, 713 (1980).

[17] K. Siegbahn *et al.*, *ESCA Applied to Free Molecules* (North-Holland, Amsterdam, 1969).

[18] W. Wurth *et al.*, Phys. Rev. Lett. **65**, 2426 (1990).

[19] T. D. Thomas and R. W. Shaw, J. Electron. Spectrosc. **5**, 1081 (1974).

[20] O. Edqvist *et al.*, Phys. Scr. **1**, 172 (1970).

[21] W. H. E. Schwartz and R. J. Buenker, Chem. Phys. **13**, 153 (1976).

[22] D. W. Davis and D. A. Shirley, J. Electron. Spectrosc. **3**, 157 (1974).

[23] F. X. Gadea *et al.*, Phys. Rev. Lett. **66**, 883 (1991).

[24] W. B. Perry and W. L. Jolly, Inorg. Chem. **13**, 1211 (1974).

[25] The two spectra in Fig. 8 are aligned by the position of peak No. 1.

[26] A. P. Hitchcock, M. Pocock, and C. E. Brion, Chem. Phys. Lett. **49**, 125 (1977); K. Randall *et al.* (unpublished).